The 4th International Conference on Control and Robotics Engineering

Motion Camouflage for Point-Mass Robots Using a Lyapunov-based Control Scheme

Avinesh Prasad
School of Computing, Information and Mathematical Sciences
University of the South Pacific
Fiji
e-mail: avinesh.prasad@usp.ac.fj

Bibhya Sharma
School of Computing, Informationand Mathematical Sciences
University of the South Pacific
Fiji
e-mail: bibhya.sharma@usp.ac.fj

Jito Vanualailai
School of Computing, Informationand Mathematical Sciences
University of the South Pacific
Fiji
e-mail: vanualailai@usp.ac.fj

***Abstract*— This article presents a new solution to the motion camouflage problem for point-mass robots using a Lyapunov-based control scheme. We consider a workspace with one shadower and one shadowee. We design our control inputs for shadower and the shadowee such that at each moment the shadower must follow the camouflage constraint line (the line that joins the instantaneous position of the shadowee with a fixed focal point). This strategy allows the shadower to appear stationary to the shadowee and will help the shadower to effectively catch the shadowee without spending much of its energy. The convergence of the two robots to a neighborhood of a pre-defined target is guaranteed by the Lyapunov's direct method. Computer simulations validate the control inputs and the effectiveness of Lyapunov-based control scheme.**

Keywords- Motion camouflage, Lyapunov-based control scheme, shadower, shadowee, camouflage constraint line.

I. INTRODUCTION

Motion camouflage is a naturally inspired behavior involving a shadower (such as a predator) and one or multiple shadowees (the preys) where the shadower, approaching a shadowee, appears stationary to the shadowee so that the latter does not effectively notice the approach of the former [1]. This behavior is common in insects and animals, and is effective for avoiding a predator, catching a prey, mating or defending an enemy.

According to motion camouflage theory, the shadower follows a trajectory such that it appears stationary from the shadowee's point of view [2]. Thus at each time $t \geq 0$, the shadower must follow the Camouflage Constraint Line (CCL) which joins the instantaneous position of the shadowee with a fixed focal point. The trajectory followed by the shadower can either approach (camoufled approach) or move away from the shadowee (retreat) [2]. In a predator-prey relationship, if the predator follows the camouflaged trajectory, it will have high chances of catching the prey even at low speed, without spending much of its energy [1]. Similarly, if the prey follows the camouflaged trajectory, then it can easily flee without the predator effectively noticing it.

Various techniques have been deployed in literature to model the motion camouflage behavior in insects and its implications in robotics. We present a few prominent ones. Mizutani et al. in [3] observed the movements of dragonflies using stereo cameras and showed that the insects actively use motion camouflage to disguise themselves as stationary during territorial aerial manoeuvres. Glendinning et al. in [1] derived the differential equations for motion camouflage and analysed some simple cases. Carey et al. [4] described and solved several types of motion camouflage behaviours within a linear quadratic Gaussian (LQG) framework and found optimal strategies for achieving the motion constraints and the overall engagement requirements. Rana and Burbridge in [2] formulated and solved the motion camouflage as a nonlinear optimal control problem. Rana and Iglesias in [5] presented the first implementation of motion camouflage in real wheeled robots through a polynomial NARMAX model controller. Zhang et al. [6] used Bayesian approach to detect camouflaged moving object. Other noteworthy contributions were made by Justh et al. [7] in 2005, Reddy et al. [8] in 2006, Galloway et al. [9] in 2007, Mischiati et al. [10] in 2012, and Li [11] in 2017.

This paper addresses the motion camouflage problem by considering two point-mass robots (one shadower and one shadowee). The motion of the two robots are modelled as a system of first-order nonlinear differential equations. We then utilize the Lyapunov-based Control Scheme to extract a set of nonlinear, time-invariant, continuous control inputs to drive the robots to the targets. Our main objective is to use the Lyapunov-based control scheme, which was proposed

978-1-7281-1593-1/19/$31.00 ©2019 IEEE

by Sharma in [12], to derive the controllers. The main idea behind the control scheme is to design an appropriate Lyapunov function which acts as an energy function. We construct attractive and avoidance functions for the attraction to targets and repulsion from various obstacles, respectively. The Lyapunov function is the sum of all attractive and repulsive potential functions. We note from [12] that the repulsive potential functions are designed as ratios with the obstacle avoidance function in the denominator of each ratio and a positive control parameter in the numerator. The control inputs are designed such that the Lyapunov function is decreasing for all $t \geq 0$ and vanishes to zero as $t \to +\infty$. Figure 1 shows the block diagram that explains th design procedure and the control structure. The reasons for utilizing this scheme is mainly due to its simplicity and elegance, the extraction of control inputs is straightforward, and the scheme easily incorporates system singularities and constraints [12].

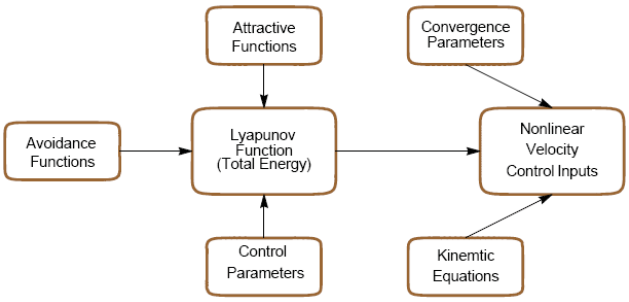

Figure 1. Block diagram explaining the Lyapunov-based control scheme.

The main contributions of this paper are:

1. Designing a new set of nonlinear, continuous velocity control inputs, which is based on the construction of a Lyapunov function that acts as an energy function of the system.
2. The control inputs are constructed such that at each moment the shadower follows the camouflage constraint line whilst it is approaching the shadowee.
3. The proposed method easily incorporates any system singularities and obstacle parameters into the control scheme.
4. In this paper, the equilirium point of the system is proved to be stable. We use the Direct Method of Lyapunov to carry out the stability analysis and theoretically show that the equilirium point is stable.

The reminder of the paper is organized as follows: The kinematic model describing the motion of the two robots is derived in Section II. In Section III, the targets are defined and the attractive potential functions are given which inherently allows the robots to converge to their targets. The potential functions for the avoidance of singular point and fixed obstacles are discussed in Section IV. Section V provides a Lyapunov function or total potentials of the system, from which, the nonlinear control inputs are designed such that the two robots must converge to the targets whilst avoiding all obstacles on their paths. Stability of the system is discussed in Section VI. Simulations results are provided in Section VII followed by conclusion and remarks on future work in Section VIII.

II. KINEMATIC MODEL

Consider the camouflage constraint line shown in Figure 2. Let the focal point be at (a,b) and let the shadowee be positioned at (x,y) at any time $t \geq 0$. Suppose the shadower is at a distance of $r(t)$ units from the focal point and at an angle of $\theta(t)$ measured counter-clockwise from the focal point, then the position of the shadower at time t is given by $\big(x_0(t),\, y_0(t)\big) = \big(a + r(t)\cos\theta(t), b + r(t)\sin\theta(t)\big)$.

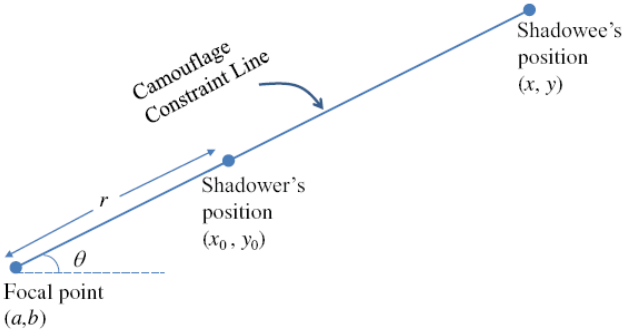

Figure 2. The camouflage constraint line.

Let $v_0 = u_{01}\mathbf{i} + u_{02}\mathbf{j}$ and $v_1 = u_{11}\mathbf{i} + u_{12}\mathbf{j}$ be the velocity of the shadower and shadowee, respectively. Then the kinematic equations relating the motions of the two objects can be expressed as

$$\left.\begin{aligned} \dot{x} &= u_{11}, \quad \dot{y} = u_{12} \\ \dot{r} &= u_{01}\cos\theta + u_{02}\sin\theta, \\ \dot{\theta} &= \frac{u_{12}\cos\theta - u_{11}\sin\theta}{\sqrt{(x-a)^2 + (y-b)^2}} \\ r(0) &= \sqrt{(x_0(0)-a)^2 + (y_0(0)-b)^2} \\ \theta(0) &= \operatorname{atan2}\,(y(0)-b,\, x(0)-a)\,. \end{aligned}\right\} \tag{1}$$

Here u_{i1} and u_{i2}, i = 0,1 are classified as the nonlinear velocity control inputs. We shall use the vector notation $\mathbf{x}(t) = \big(x(t), y(t), r(t), \theta(t)\big) \in \mathbb{R}^4$ to refer to the positional configurations of the two point-mass robots. We further note that $(x-a)^2 + (y-b)^2 = 0$ produces a singular point since $\dot{\theta} \to +\infty$ as $(x-a)^2 + (y-b)^2 \to 0$. Later in Section IV, we will treat this as an artificial obstacle to avoid this singularity.

III. TARGETS

Let's fix a target for the shadowee to reach after some time t. The target is a circular disk with center (p_1, p_2) and radius r_T described as

$$T = \left\{(z_1,\, z_2) \in \mathbb{R}^2 : (z_1 - p_1)^2 + (z_2 - p_2)^2 \le r_T^2\right\}.$$

Next, we want the shadower to be attracted to the shadowee. Hence (x, y) will act as a moving target for the shadower. For attractions to the targets, we consider the following attractive potential functions

$$V_1(\mathbf{x}) = \frac{1}{2}\left[(a + r\ \cos\theta - x)^2 + (b + r\sin\theta - y)^2\right], \quad (2a)$$

$$V_2(\mathbf{x}) = \frac{1}{2}\left[(x - p_1)^2 + (y - p_2)^2\right], \quad (2b)$$

We shall see later that when the total energy function is designed, $V_1(\mathbf{x})$ will act as an attractive potential function, attracting the shadower towards the shadowee. Similarly, $V_2(\mathbf{x})$ will act as an attractive potential function, attracting the shadowee to its designated target.

IV. OBSTACLES

As seen in system (1), $(x-a)^2 + (y-b)^2 = 0$ produces a singular point. To avoid this singularity, we consider an obstacle avoidance function

$$S(\mathbf{x}) = \frac{1}{2}\left[(x-a)^2 + (y-b)^2\right], \quad (3)$$

We will see later that the avoidance function $S(\mathbf{x})$ will be added as a ratio to a Lyapunov function of the system. Note that along any trajectories generated by system (1), a Lyapunov function, say, $L(\mathbf{x}(t))$, is always non-negative and decreasing for all $t \ge 0$. Hence $L(\mathbf{x}(t)) \le L(\mathbf{x}(0)) < \infty$. Now consider the effect of the ratio $\gamma / S(\mathbf{x})$ for some constant $\gamma > 0$. When $(x-a)^2 + (y-b)^2 \to 0$, this ratio will increase making $L(\mathbf{x}(t)) \to \infty$. This cannot happen since $L(\mathbf{x}(t))$ is a decreasing function and $L(\mathbf{x}(t)) < \infty$. Thus we conclude that $S(\mathbf{x}) > 0$ and the singular point will always be avoided.

Let us also fix $q \in \mathbb{N}$ circular obstacles within the workspace. The lth obstacle (for $l = 1,2,\ldots,q$) is a disk with center (o_{l1}, o_{l2}) and radius ro_l and is defined as the set

$$FO_l = \left\{(z_1,\, z_2) \in \mathbb{R}^2 : (z_1 - o_{l1})^2 + (z_2 - o_{l2})^2 \le ro_l^2\right\}$$

For the avoidance of these fixed obstacles by the shadowee and shadower, we construct the potential functions

$$W_{1l}(\mathbf{x}) = \frac{1}{2}\left[(a + r\ \cos\theta - o_{l1})^2 + (b + r\sin\theta - o_{l2})^2 - ro_l^2\right], \quad (4a)$$

$$W_{2l}(\mathbf{x}) = \frac{1}{2}\left[(x - o_{l1})^2 + (y - o_{l2})^2 - ro_l^2\right], \quad (4b)$$

for $l = 1,2,\ldots,q$. Again, for the avoidance of the fixed obstacles, the potential functions $W_{il}(\mathbf{x})$ ($l = 1,2,\ldots,q$ and i = 1, 2) will be added as a ratio to a Lyapunov function of the system.

V. CONTROL INPUTS

We define a Lyapunov function (total energy) from which we will extract the control inputs. Combining all the attractive and repulsive potential functions and introducing *control parameters*, $\alpha_i > 0$, $\beta_{il} > 0$ and $\gamma > 0$, we define a Lyapunov function for system (1) as

$$L(\mathbf{x}) = \sum_{i=1}^{2}\left[\alpha_i V_i(\mathbf{x}) + \sum_{l=1}^{q}\frac{\beta_{il} V_i(\mathbf{x})}{W_{il}(\mathbf{x})}\right] + \frac{\gamma V_2(\mathbf{x})}{S(\mathbf{x})} \quad (5)$$

which is defined, continuous and positive over the domain

$$D = \{\mathbf{x} \in \mathbb{R}^4 : S(\mathbf{x}) > 0; W_{il}(\mathbf{x}) > 0,\ l = 1,\ldots,\ q,\ i = 1,2\}.$$

To extract the control inputs for system (1), we differentiate the various components of $L(\mathbf{x})$ separately with respect to t to obtain (on suppressing $\mathbf{x}$)

$$\begin{aligned}\dot{L}(\mathbf{x}) &= \frac{\partial L}{\partial x}\dot{x} + \frac{\partial L}{\partial y}\dot{y} + \frac{\partial L}{\partial r}\dot{r} + \frac{\partial L}{\partial \theta}\dot{\theta} \\ &= \frac{\partial L}{\partial r}u_{01}\cos\theta + \frac{\partial L}{\partial r}u_{02}\sin\theta \\ &\quad + \left(\frac{\partial L}{\partial x} - \frac{\partial L}{\partial \theta}\frac{\sin\theta}{\sqrt{2S}}\right)u_{11} + \left(\frac{\partial L}{\partial y} + \frac{\partial L}{\partial \theta}\frac{\cos\theta}{\sqrt{2S}}\right)u_{12}\end{aligned}$$

Given the convergence parameters $\delta_j > 0$ for j = 1, 2, 3, 4, we let the velocities to have the form

$$\begin{aligned}-\delta_1 u_{01} &= \frac{\partial L}{\partial r}\cos\theta \\ -\delta_2 u_{02} &= \frac{\partial L}{\partial r}\sin\theta \\ -\delta_3 u_{11} &= \frac{\partial L}{\partial x} - \frac{\partial L}{\partial \theta}\frac{\sin\theta}{\sqrt{2S}} \\ -\delta_4 u_{12} &= \frac{\partial L}{\partial y} + \frac{\partial L}{\partial \theta}\frac{\cos\theta}{\sqrt{2S}}\end{aligned}$$

then along a trajectory of system (1) in D, we have

$$\dot{L}(\mathbf{x}) = -\delta_1 u_{01}^2 - \delta_2 u_{02}^2 - \delta_3 u_{11}^2 - \delta_4 u_{12}^2 \le 0$$

provided our feedback nonlinear controllers are of the form

$$\left.\begin{aligned}u_{01} &= -\frac{1}{\delta_1}\frac{\partial L}{\partial r}\cos\theta \\ u_{02} &= -\frac{1}{\delta_2}\frac{\partial L}{\partial r}\sin\theta \\ u_{11} &= -\frac{1}{\delta_3}\left(\frac{\partial L}{\partial x} - \frac{\partial L}{\partial \theta}\frac{\sin\theta}{\sqrt{2S}}\right) \\ u_{12} &= -\frac{1}{\delta_4}\left(\frac{\partial L}{\partial y} + \frac{\partial L}{\partial \theta}\frac{\cos\theta}{\sqrt{2S}}\right)\end{aligned}\right\} \quad (6)$$

VI. Stability of System (1)

We note that the controllers u_{01}, u_{02}, u_{11} and u_{12} defined in (6) are continuous on the domain D. If we let

$$r^* = \sqrt{(p_1 - a)^2 + (p_2 - b)^2} \text{ and}$$

$$\theta^* = \text{atan2}(p_2 - b,\ p_1 - a) + 2\pi n \text{ for some } n \in \mathbb{N}$$

then $\mathbf{x}_e = (p_1, p_2, r^*, \theta^*)$ is an equilibrium point of system (1). Now since the Lyapunov function $L(\mathbf{x})$ of system (1) is defined, continuous and positive over the domain

$$D = \{\mathbf{x} \in \mathbb{R}^4 : S(\mathbf{x}) > 0; W_{il}(\mathbf{x}) > 0,\ l = 1, \ldots, q,\ i = 1, 2\}.$$

it can easily be verified that $L(\mathbf{x})$ satisfies the following properties:

1. $L(\mathbf{x})$ is continuous and has first partial derivatives in the region D in the neighborhood of the point $\mathbf{x}_e$ of system (1);
2. $L(\mathbf{x}_e) = 0$;
3. $L(\mathbf{x}) > 0$ for all $\mathbf{x} \in D \setminus \mathbf{x}_e$;
4. $\dot{L}(\mathbf{x}) \le 0$ for all $\mathbf{x} \in D$;
5. $\dot{L}(\mathbf{x}_e) = 0$

Hence $L(\mathbf{x})$ is a Lyapunov function of system (1) that guarantees its stability and we conclude that the equilibrium point $\mathbf{x}_e$ of system (1) is stable provided the controllers u_{01}, u_{02}, u_{11} and u_{12} are as defined in (6).

VII. Simulations

In this section, we demonstrate computer simulations of our proposed technique. The three scenarios given in this section capture realistic situations to illustrate the effectiveness and robustness of the velocity-based controllers and the control scheme.

A. *Scenario 1*

In this scenario, we consider a simple set up (without any fixed obstacles) where the shadowee moves from an initial position to a pre-defined target. The shadower then moves towards the shadowee by closely following the constant camouflage line (CCL) as seen in Figure 3. The CCL at various time is shown in the figure. We note that the distance between the shadower and the shadowee decreases as the two robots move along their trajectories. Finally, the shadower is able to converge on the shadowee at the shadowee's target. The initial and final positions and other simulation details are given below.

1. Initial state: $(x(0), y(0), r(0), \theta(0)) = (25, 0, 10, 0)$.
2. Shadowee's target: $(p_1, p_2) = (20, 25)$.
3. Focal point: $(a, b) = (0, 0)$.
4. Convergence parameters: $\delta_j = 10$ for $j = 1, 2, 3, 4$.
5. Control parameters: $\alpha_1 = 1$, $\alpha_2 = 1$ and $\gamma = 0.1$.

Figure 4 shows the evolution of the Lyapunov function and its time derivative along the trajectories shown in Figure 3. One can clearly notice that Lyapunov function is continuous, positive, strictly decreasing and vanishes as $t \to +\infty$.

B. *Scenario 2*

In this scenario, we have placed a circular fixed obstacle, positioned at $(o_{11}, o_{12}) = (10, 17)$ with radius $ro_1 = 2$, within the workspace for the two robots to avoid along their paths. The robots clearly avoid the obstacle while following the camouflage constraint line and converge nicely to the

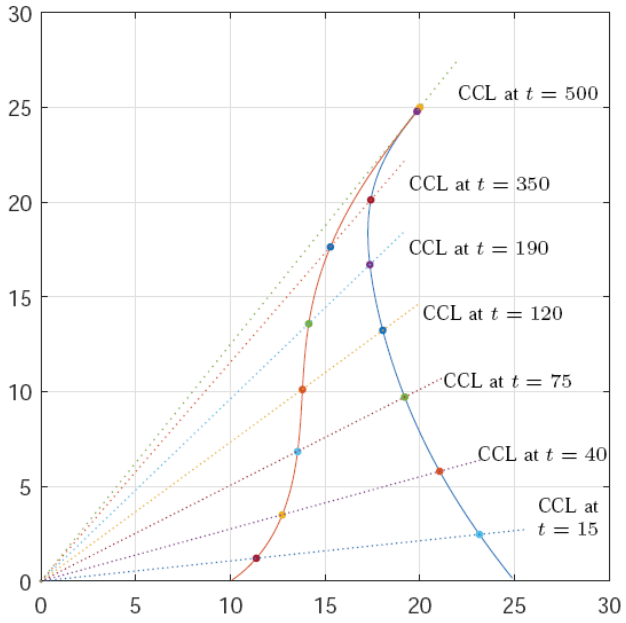

Figure 3. Path followed by the shadowee (in blue) and shadower (in brown) in a workspace without fixed obstacles.

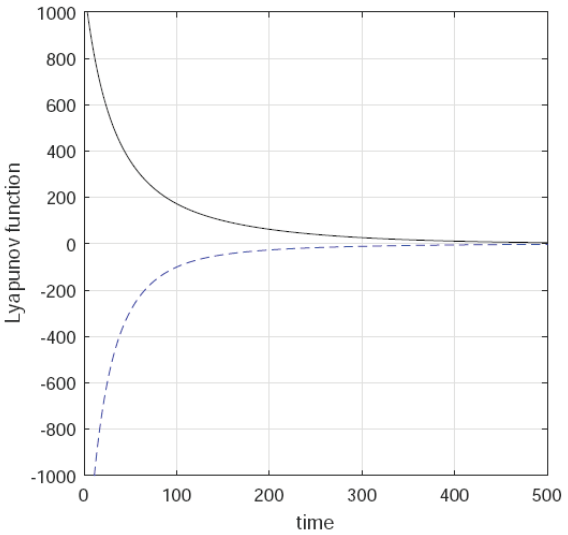

Figure 4. Evolution of the Lyapunov function (in black) and its time derivative (in blue) along the trajectories in Figure 3.

targets as shown in Fig. 5. The initial state and shadowee's target position is given in the figure caption while the other values were kept same as in Scenario 1. The evolution of the Lyapunov function and its time derivative along the trajectories is depicted in Fig. 6. The almost flat portion of the graph of $L(\mathbf{x})$ indicate indicates the time interval in which the robots avoid the fixed obstacle.

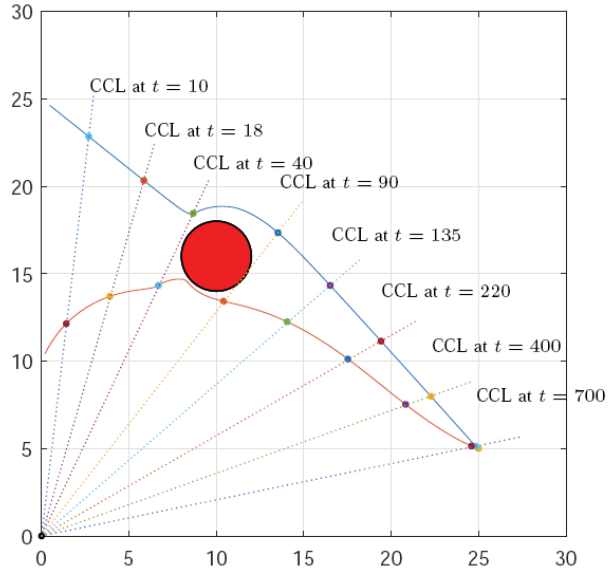

Figure 5. Path followed by the shadowee (in blue) and shadower (in brown) with initial state $(x(0), y(0), r(0), \theta(0)) = (0, 25, 10, \frac{\pi}{2})$ and shadowee's target placed at $(p_1, p_2) = (25, 5)$.

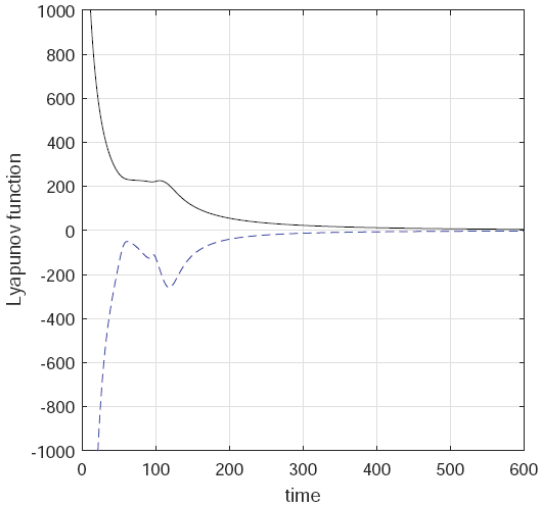

Figure 6. Evolution of the Lyapunov function (in black) and its time derivative (in blue) along the trajectories in Figure 5.

VIII. Concluding Remarks

In this paper, a new solution to the motion camouflage problem for point-mass robots is presented. The Lyapunov-based control scheme was applied to derive continuous control inputs involving one shadower and one shadowee such that at each moment the shadower must follow the camouflage constraint line while avoiding any fixed obstacle along its path.

The convergence of the two robots to a neighborhood of a pre-defined target is guaranteed by the Lyapunov's direct method. Computer simulations were used to illustrate the effectiveness of our control scheme. The velocity-based nonlinear control inputs proposed also take into account the singular point associated with the system.

Future work in this area includes solving the motion camouflage problem involving multiple shadowers and shadowees in two and three dimensional workspace. Moreover, partially known or fully unknown workspace, where the positions, sizes and geometry of obstacles may be unknown, will be an interesting but challenging research to consider in future.

References

[1] P. Glendinning, "The mathematics of motion camouflage," in *Proceedings of Biological Sciences*, vol. 271, no. 1538, pp. 477–481.

[2] I. Rano and C. Burbridge, "Motion camouflage for unicycle robots using optimal control," in Proceedings of Towards Autonomous Robotic Systems (TAROS).

[3] A. Mizutani, J. S. Chahl, and M. V. Srinivasan, "Insect behaviour: Motion camouflage in dragonflies," *Nature*, vol. 423, pp. 604–604, 2003.

[4] N. E. Carey, J. J. Ford, and J. S. Chahl, "Biologically inspired guidance for motion camouflage," in *5th Asian Control Conference*, vol. 3, July 2004, pp. 1793–1799.

[5] I. Rano and R. Iglesias, "Application of systems identification to the implementation of motion camouflage in mobile robots," *Autonomous Robots*, vol. 40, no. 2, pp. 229–244, 2016.

[6] X. Zhang, C. Zhu, S. Wang, Y. Liu, and M. Ye, "A bayesian approach to camouflaged moving object detection," *IEEE Transactions on Circuits and Systems for Video Technology*, vol. 27, no. 9, pp. 2001–2013, Sep. 2017.

[7] W. Justh and P. S. Krishnaprasad, "Steering laws for motion camouflage," 2005.

[8] P. V. Reddy, E. W. Justh, and P. K. Krishnaprasad, "Motion camouflage in three dimensions," Proceedings of the 45th IEEE Conference on *Decision and Control*, pp. 3327–3332, 2006.

[9] K. S. Galloway, E. W. Justh, and P. S. Krishnaprasad, "Motion camouflage in a stochastic setting," *in 2007 46th IEEE Conference on Decision and Control*, Dec 2007, pp. 1652–1659.

[10] M. Mischiati and P. Krishnaprasad, "The dynamics of mutual motion camouflage," *Systems & Control Letters*, vol. 61, no. 9, pp. 894 – 903, 2012.

[11] W. Li, "A dynamics perspective of pursuit-evasion: Capturing and escaping when the pursuer runs faster than the agile evader," *IEEE Transactions on Automatic Control*, vol. 62, no. 1, pp. 451–457, Jan 2017.

[12] B. Sharma, "New directions in the applications of the Lyapunov-based control scheme to the findpath problem," Ph.D. dissertation, University of the South Pacific, Suva, Fiji Islands, July 2008.